Activation of oxygen-responsive pathways are associated with altered protein metabolism in Arctic char exposed to hypoxia

Alicia A. Cassidy and Simon G. Lamarre

Département de Biologie, Université de Moncton, Moncton, NB, Canada

Corresponding author: Alicia A. Cassidy

alicia.cassidy@umoncton.ca

Keywords: Hypoxia, Protein Degradation, HIF, Unfolded Protein Response, mTOR, Arctic char

Abstract

Fish exposed to fluctuating oxygen concentrations often alter their metabolism and/or behaviour to survive. Hypoxia tolerance is typically associated with the ability to reduce energy demand by supressing metabolic processes such as protein synthesis. Arctic char is amongst the most sensitive salmonid to hypoxia, and typically engage in avoidance behaviour when faced with lack of oxygen. We hypothesized that a sensitive species will still have the ability (albeit reduced) to regulate molecular mechanisms during hypoxia. We investigated the tissue-specific response of protein metabolism during hypoxia. Little is known on protein degradation pathways during hypoxia in fish and we predict that protein degradation pathways are differentially regulated and play a role in the hypoxia response. We also studied the regulation of oxygen-responsive cellular signalling pathways (Hypoxia inducible factor, unfolded protein response and mTOR pathway) since most of what we know comes from studies on cancerous mammalian cell lines.

Arctic char, were exposed to a cumulative, graded hypoxia trials, for 3 hours at each air saturation level (100%, 50%, 30% and 15%). The rate of protein synthesis was measured using a flooding dose technique, while protein degradation and signalling pathways were assessed by measuring transcripts and phosphorylation of target proteins. Protein synthesis decreased in all tissues measured (liver, muscle, gill, digestive system) except for the heart. Salmonid hearts have preferential access to oxygen through a well-developed coronary artery, therefore the heart is likely the last tissue to become hypoxic. Autophagy markers were upregulated in the liver, while protein degradation markers were downregulated in the heart during hypoxia. Further work is needed to determine the effects of a decrease in protein degradation on a hypoxic salmonid heart. Our study showed that protein metabolism in Arctic char is altered in a tissue-specific fashion during graded hypoxia, which is in accordance with the responses of the three major hypoxia-sensitive pathways (HIF, UPR and mTOR). The activation pattern of these pathways and the cellular processes that are under their control varies greatly among tissues, sometimes even going in opposite direction. This study provides new insights on the effects of hypoxia on protein metabolism. The adjustments of these cellular processes likely contribute in shifting the fish phenotype into a more hypoxia tolerant one, if more than one hypoxia event were to occur. Our results warrant studying these adjustments in fish exposed to long-term and diel cycling hypoxia.

Abbreviations

4EBP1	eukaryotic Translation Initiation Factor 4E-Binding Protein 1
AKT	protein kinase B
AMPK	5' AMP-activated protein kinase
ATF4	Activating Transcription Factor 4
ATG4	Autophagy Related 4A Cysteine Peptidase
BNIP3	BCL2/adenovirus E1B 19-kD protein-interacting protein 3
DDIT3	DNA-Damage-Inducible Transcript 3
eif2α	eukaryotic translation initiation factor 2α
FbxO25	F-box only protein 25
FOXO	forkhead box O
HIF	hypoxia inducible factor
K_S	Fractional rate of protein synthesis
LC3B	Microtubule Associated Protein 1 Light Chain 3 Beta
mTOR	mammalian target of rapamycin)
P70S6K	ribosomal protein S6 kinase beta-1
REDD1	regulated in development and DNA damage responses 1
UBE2H	ubiquitin conjugating enzyme E2 H
UPR	unfolded protein response
TSC1-TSC2	hamartin–tuberin protein complex
VEGF	vascular endothelial growth factor
VHL	von Hippel–Lindau

Introduction

Fish are regularly exposed to fluctuations in oxygen concentrations in the wild, often associated with increased water temperature and eutrophication. The ability to tolerate hypoxia varies between species and individuals, and depends on a fish's capacity to alter its behaviour and/or physiology when oxygen levels decrease (Farrell and Richards, 2009; Richards, 2010). Different species employ a wide range of strategies to increase survival during hypoxia, including increasing gill ventilation and cardiac output to enhance oxygen extraction from the environment (Farrell and Richards, 2009; Richards, 2010). Hypoxia-tolerant species such as crucian carp (*Carassius carassius*), oscars (*Astronotus ocellatus*) and goldfish (*Carassius auratus*) lower their metabolic rate to limit the use of anaerobic metabolism and the accumulation of toxic end-products (reviewed in Boutilier, 2001; Lewis et al., 2007). This is accomplished by suppressing energetically expensive processes such as reproduction, digestion and growth (Boutilier, 2001; Farrell and Richards, 2009).

Metabolic suppression during hypoxia can be partially accomplished by suppressing protein metabolism, which includes both protein synthesis and protein degradation. Hypoxia-tolerant species, such as the Amazonian oscar and crucian carp can suppress protein synthesis by as much as 95% in liver and 55% in muscle (Cassidy et al., 2018; Lewis et al., 2007; Smith et al., 1996) during hypoxia, accounting for a 20-36% decrease in metabolism (Cassidy et al., 2018). The adjustments of protein metabolism, if any, have not yet been characterized in hypoxia-sensitive species such as salmonids. Regulation of protein synthesis during hypoxia is well documented in mammals and is starting to be characterized in fish, yet there is little information on regulation of protein degradation. In mammals, the autophagy pathway is activated during hypoxia (Wouters and Koritzinsky, 2008), with little information on the other protein degradation pathways (ubiquitin proteasome pathway and calpains).

There are three major cellular signalling pathways involved in the hypoxia response; the hypoxia inducible factor (HIF) pathway, the unfolded protein response (UPR) and mTOR pathway (Cassidy et al., 2018; Fang et al., 2015; Wouters and Koritzinsky, 2008). When activated, these pathways eventually inhibit the rate of protein synthesis (Wouters & Koritzinsky, 2008; summarized in Fig. 1). The responses of these pathways are well characterized in mammalian

tumours and are starting to be elucidated in fish exposed to hypoxia. During hypoxia, HIF-1α accumulates in cells and dimerizes with HIF-β which promotes the expression of genes involved in various processes such as angiogenesis and glycolysis (Neufeld et al., 1999; Schofield and Ratcliffe, 2004). HIF may also control the rate of protein synthesis through transcriptional regulation of BNIP3 and REDD1, which inhibit mTOR and protein synthesis (Wouters and Koritzinsky, 2008). In fish, *HIF* transcripts increase during hypoxia and its function during hypoxia appears conserved in fish (Baptista et al., 2016; Heinrichs-Caldas et al., 2019; Rimoldi et al., 2012; Shen et al., 2010). The UPR is activated by an accumulation of unfolded or misfolded proteins in the endoplasmic reticulum (ER) during hypoxia. Its primary functions include degrading misfolded proteins and inhibiting protein synthesis to limit the accumulation of misfolded proteins in the ER (Zhang and Kaufman, 2006). Briefly, PERK (protein kinase RNA-like endoplasmic reticulum kinase) is activated by autophosphorylation and phosphorylates eIF2α, which directly inhibits translation initiation and, therefore, protein synthesis (Ron and Walter, 2007). The phosphorylation of eiF2α during hypoxia was reported in the Amazonian oscar (Cassidy et al., 2018), and transcriptional activation of its downstream targets were reported in the common sole (*Solea solea*) (Mazurais et al., 2014), suggesting that this pathway is also conserved in fish. Finally, the mTOR pathway regulates, among other things, both protein synthesis and degradation in response to various effectors such as hypoxia, food availability or pathogens (Fader et al., 2015; Hay and Sonenberg, 2004; Johnston et al., 2011). mTOR phosphorylates its downstream targets, 4EBP1 and P70S6K, which directly regulate global protein synthesis (Hay and Sonenberg, 2004). During hypoxia in mammals, mTOR is regulated by multiple pathways, including HIF-dependent, and HIF-independent pathways that involve AMPK (Liu et al., 2006; Papandreou et al., 2008). AMPK is an energy sensor that regulates multiple cellular processes including glucose and protein metabolism. AMPK is activated during severe hypoxia, and its activation inhibits mTOR activity, thus inhibiting protein synthesis (Cam and Houghton, 2011; Mungai et al., 2011; Papandreou et al., 2008). There is limited information on the regulation of the mTOR pathway during hypoxia in fish. However, AMPK phosphorylation increased in goldfish and rainbow trout exposed to hypoxia, suggesting that mTOR pathway should also be inhibited (Jibb and Richards, 2008; Williams et al., 2019). In mammals, there is also significant crosstalk between the three hypoxia response pathways and each one (HIF, UPR or mTOR) can regulate the activity of one of the other pathways (Wouters and Koritzinsky, 2008).

Protein degradation is also regulated by hypoxia responsive signalling pathways, although less is known on the regulation of the three major protein degradation pathways (autophagy, ubiquitin proteasome pathway and calpains) during hypoxia. Autophagy and the ubiquitin proteasome pathway are both controlled by cell signalling pathways, including the AKT/mTOR pathway (Johnston et al., 2011). During hypoxia, autophagy is activated by all three hypoxia response pathways (HIF, UPR and mTOR) in mammals (Wouters and Koritzinsky, 2008). It is not known, however, whether the ubiquitin proteasome pathway or the calpain system are also regulated by hypoxia response pathways such as HIF or UPR. Autophagy is responsible for degrading organelles and proteins with long half-lives and includes acidic proteases called cathepsins that degrade proteins and organelles inside vacuoles (Ciechanover, 2012). It is not known whether autophagy is regulated during hypoxia in fish, but a recent study linked autophagy and hypoxia in prawn (*Macrobrachium nipponense*) hepatocytes (Sun et al., 2019). The ubiquitin proteasome pathway is mostly responsible for degrading damaged proteins, and proteins with short half-lives (Glickman and Ciechanover, 2002). This pathway involves three groups of enzymes that tag proteins with a poly-ubiquitin chain that will then be recognized and degraded by the proteasome complex (Ciechanover et al., 1984). In mammals, one study observed a decrease in proteasome activity during hypoxia (Gozal et al., 2003), which is in accordance with a decrease in proteasome subunit transcripts observed in stickleback (*Gasterosteus aculeatus, L*) (Leveelahti et al., 2011). The third important degradation pathway is the calpain system. Calpains are small, calcium-dependent, proteases that selectively degrade proteins in the cytosol, especially in muscle (Goll et al., 2003). Calpain activity is thought to increase in mammals during hypoxia (Cui et al., 2015; Nanduri et al., 2009), however this has yet to be evaluated in fish.

Our objective was to determine whether and how protein metabolism is deregulated in tissues of Arctic char submitted to cumulative, graded hypoxia trials. The hypotheses were that (1) as observed in hypoxia-tolerant species, protein metabolism is regulated during hypoxia in an attempt to maintain energy homeostasis and that this regulation is carried by the aforementioned hypoxia responsive pathways. (2) The reorganization of protein metabolism during hypoxia differs among tissues that have drastically different metabolic rates and functions (i.e. liver, white muscle and cardiac muscle). Unlike many cyprinids that tolerate low-oxygen environments, salmonids require higher oxygen availability (Jones et al., 2008). Arctic char, *Salvelinus alpinus*, is the

northernmost freshwater fish species, and is considered amongst the most hypoxia-sensitive salmonid (Jones et al., 2008). This low hypoxia tolerance makes Artic char a good model to study the effects of hypoxia on protein metabolism and to study which hypoxia responsive pathways are involved in fish tissues.

Arctic char were exposed to a protocol of graded decreases in air saturation (three hours at each of 100%, 50%, 30% and then 15% air saturation) and we measured the fractional rate of protein synthesis and indicators of protein degradation in the liver, white muscle and heart at each oxygen concentration. We found profound alterations of the rate of protein synthesis and the abundance of various markers of protein degradation, but these were highly tissue specific.

Materials and methods

Rearing conditions and experimental design

Juvenile Arctic char (Fraser strain; body mass = 60.9 g ± 1.6, s.e.m.) were obtained from the Coastal Zones Research Institute Inc. (Shippagan, NB, Canada). Five hundred fish were held in two 250 L tanks supplied with flow-through dechlorinated freshwater. Fish were fed a commercial salmon diet (Corey Nutrition Company Inc., Fredericton, NB, Canada) at 2% body weight per day, every other day. Water temperatures varied seasonally and was 16°C in the summer, when the experiment occurred.

The experimental system consisted of three shelves each containing six 9 L tanks. Each shelf had its own water filtration and biofiltration system. The dissolved oxygen was adjusted by nitrogen injection by means of a programmable proportional–integral–derivative controller (Aquabiotech, Coaticook, Qc, Canada). Temperature was maintained at 16 ± 0.1°C. In June 2017, fish were semi-randomly selected (excluding the runts) and transferred to experimental tanks over the span of 5 days. Fish were feed-deprived for 4 days before the experiment. Twenty fish (5 per group) were exposed to a cumulative, graded hypoxic challenge, with an endpoint of either 100%, 50%, 30% or 15% air saturation (Fig. 2) as in Cassidy et al (2018). Five fish (1 per tank) were placed in the experimental chambers overnight at 100% air saturation for acclimation and sampled the next day (control group). The next day, 5 additional fish were placed in the chambers overnight

at 100% air saturation for acclimation. Air saturation was then dropped to 50%, and maintained at 50% for 3 hours before sampling. A third group of 5 fish were then placed in the tanks overnight at 100% air saturation. Air saturation levels were then dropped to 50% for 3 hours the following morning, then held at 30% for 3 hours before sampling. The last group of fish was placed in the tanks overnight at 100% air saturation. The next morning, air saturation levels dropped to 50% for 3 hours, then 30% for 3 hours and finally 15% for 3 hours before sampling. We did not expose fish to oxygen concentrations lower than 15% since at this level fish were starting to lose equilibrium. Oxygen concentration measured by the system was always confirmed using a handheld oxygen meter (5512-Ft YSI, USA, Ohio, Yellow Springs). At the end of each hypoxic challenge, fish were killed by severing the spinal cord directly behind the brain. Blood was immediately collected from the caudal vein, centrifuged 5 minutes at 2000 *g* and the plasma frozen. Samples of muscle, liver, heart, gill and blood were collected and immediately frozen in liquid nitrogen. Samples were then stored at -80°C until further analysis. Experiments were conducted with the approval of the animal care committee at the Université de Moncton, New Brunswick, Canada (UdeM17-05).

Lactate

Lactate was measured in plasma, muscle and liver by first deproteinizing tissues with 6% perchloric acid followed by neutralization with 2 $mol \cdot L^{-1}$ $KHCO_3$. Lactate was measured in glycine buffer (320 $mmol \cdot L^{-1}$ glycine, 320 $mmol \cdot L^{-1}$ hydrazine, 2.4 $mmol \cdot L^{-1}$ NAD^+, with subsequent treatment of excess lactate dehydrogenase (2 $U \cdot mL^{-1}$) (Brandt et al., 1980). Absorbance was read with a multimode plate reader (Varioskan Flash, Thermo Fisher Scientific, Inc., Waltham, MA USA) at a 340 nm wavelength.

Fractional rate of protein synthesis (k_s)

The fractional rate of protein synthesis (k_s) was measured using a flooding dose technique (Garlick et al., 1980) as described and validated for this species (Cassidy et al., 2016; Lamarre et al., 2015). Fish are injected with a solution of 150 $mmol \cdot L^{-1}$ phenylalanine containing 50% [D_5]-L-phenylalanine (ring-[D_5]-PHE, 98%, Cambridge Isotope Laboratories, Inc. Andover, MA, USA), at a dosage of 1 mL per 100 g of fish body mass. Fish were injected 3 hours prior to sampling, which is an incorporation time in the optimal range, previously tested by Lamarre et al.

(2015)(Lamarre et al., 2015). Approximately 60 mg of tissue (but only 20 mg for heart) was homogenized in 1 mL of 0.2 mol·L^{-1} perchloric acid using a sonicating homogenizer (Q55 Sonicator, Qsonica Inc.). Following a 5 min 15 000 *g* centrifugation at 4°C, the supernatant containing the free amino acid pool was transferred to a new tube and kept at 4°C. The remaining protein pellet was washed three times in 1 mL of 0.2 mol·L^{-1} PCA and once in acetone. Samples were then hydrolyzed in 6 mL of 6 mol·L^{-1} HCl at 110°C for 18 hours. Phenylalanine was extracted using solid phase extraction (Bond-Elut C-18, Varian Inc.), and dried. Samples were then derivatized with pentafluorobenzyl bromide and the [D_5]-PHE enrichment of the phenylalanine from the free and protein pools were measured by GC-MS as previously described (Lamarre et al., 2015). The fractional rate of protein synthesis (K_s %·day^{-1}) is calculated using

$$K_s = \frac{S_b}{S_a} \times \frac{1440}{t} \times 100 \quad (1),$$

where S_b is the enrichment of the protein pool, S_a is the enrichment of the free amino acid pool, t is the incorporation time (min) and 1440 is the conversion from minute to day (Lamarre et al., 2015).

Immunoblots

Western blots were used to analyze specific protein levels in liver, muscle and heart. Tissues were homogenized in 9 volumes of lysis buffer (50 mmol·L^{-1} Tris, 0.1 mmol·L^{-1} EDTA, 1.0 mmol·L^{-1} β-mercaptoethanol, pH 8) with a sonicating homogenizer and centrifuged at 13 000 *g* for 15 minutes at 4°C. Protein concentration was then measured (Bradford protein assay, Bio-Rad, Hercules, CA) (Bradford, 1976). Fifteen mg of protein was loaded in each well and resolved in a 10% SDS-PAGE, transferred to PVDF membranes (Millipore, Bedford, MA), and blocked one hour with 5% BSA dissolved in TBS. Membranes were probed overnight at 4°C in primary antibodies (Cell Signalling Technologies, Beverley, MA, USA): 4EBP1 (no. 9649), p-4EBP1 (Thr 37/46; no. 2855), eIF2α (no. 5324) and p-eIF2α (ser51; no. 3398), AMPKα (no. 5831), p-AMPKα (Thr172; no. 2535). Protein bands were revealed by probing for an hour with a secondary antibody (HRP-conjugated goat anti-rabbit antibody (no. 7074) followed by enhanced chemiluminescence (Clarity Western ECL substrate, Bio-Rad, Hercules, CA). Images were taken with a Chemidoc

Touch Imaging System (Bio-Rad). The densitometric analyses were performed using Image Lab 5.2.1 software (Bio-Rad). Levels of phosphorylation were obtained by calculating the ratio between phosphorylated and total proteins (e.g., phospho-eIF2α/total eIF2α). Protein bands were normalized using the stain-free imaging technology (Gürtler et al., 2013). The relative quantity of polyubiquitinated proteins was determined by dot blots using an antibody detecting polyubiquitinated proteins (mAB, FK1, Enzo, BML-PW8805) and an anti-mouse IgM HRP linked antibody (ab97230, Abcam, Cambridge, MA) as previously described (Cassidy et al., 2016).

RNA extraction and qPCR amplification of mRNAs

Transcripts related to the hypoxia response and protein degradation were amplified *via* qPCR in liver, muscle and heart. Approximately 50 mg of tissue (15 mg for heart) were homogenized in 1 mL of TRI Reagent (Sigma-Aldrich, St. Louis, MO) with a TissueLyser (Qiagen,Venlo, Netherlands) and 5 mm stainless steel beads for 5 minutes at 27 Hz. RNA was quantified by UV absorption at 260 nm using a NanoVue spectrophotometer (GE Healthcare, Chicago, IL). RNA was treated with a DNA-free kit (Life Technologies, Carlsbad, CA) and then reverse transcribed with qScript cDNA SuperMix (Quanta Biosciences Inc., Gaithersburg, MD). Primers were designed with Primer3 (v.0.4.0) (Koressaar and Remm, 2007; Untergasser et al., 2012) using Atlantic salmon (*Salmo salar*) gene sequences obtained on NCBI (http://www.ncbi.nlm.nih.gov/) (Table S1). Gene sequences were aligned with zebrafish (*Danio rerio*) and mice (*Mus musculus*) to obtain the most conserved regions of the genes using Mega7 software(Kumar et al., 2016). Primers were validated by sequencing the PCR products (Centre de Recherche du CHUL at Université Laval) and using BLAST (NCBI) searches. qPCR assays were conducted with CFX Connect Real-Time PCR Detection System (Bio-Rad) and respected the Minimum Information for Publication of Quantitative Real-Time PCR experiments guidelines (Bustin et al., 2009). Amplification efficiencies were assessed for each tissue. Triplicates of qPCR reactions contained 5 µl of SsoAdvanced Universal SYBR Green Supermix (Bio-Rad), 4 µl of cDNA, 400 nM of forward and reverse primers and RNase-free water to a final volume of 10 µl. Data were normalized by integrating the geometric average of the 3 most stable reference genes into the Pfaffl equation (Pfaffl, 2001; Vandesompele et al., 2002). *E1fα*, *α-tubulin*, and *rs11* were the most stable reference genes in liver, *E1fα*, *β-actin* and *rs11* were selected in muscle, and in

heart, *E1fα*, *β-actin* and *α-tubulin* were selected. Normalized mRNA values are expressed relative to the average of the control group.

Statistical analyses

Linear models (*lm* function) with air saturation levels as the fixed factor (one-way ANOVA) and Tukey's *post hoc* were performed in R (CRAN, Vienna Austria) statistical software. Box-cox transformations were applied when needed, to improve the normality of the residuals. P-values smaller than 0.05 were considered statistically significant. The figures were constructed with Prism 7 software (GraphPad Software Inc.).

Results

Graded hypoxia treatment

No mortalities were observed during the cumulative, graded hypoxia treatments although a few fish started losing equilibrium at 15% air saturation. Lactate concentration in plasma and liver showed a gradual increase ($p<0.001$, $n=5$) as % air saturation levels decreased (Fig. 3. In muscle, a higher concentration of lactate only occurred at 15% oxygen saturation ($p<0.001$, $n=5$). Lactate concentration was omitted in the heart due to limited tissue availability.

Protein synthesis

The fractional rate of protein synthesis was measured in gill, liver, digestive system, white and red muscle, and heart of fish at each stage of hypoxia (Fig. 4). In most tissues, protein synthesis decreased with % air saturation except heart (Fig. 4F). The liver and digestive system were the most responsive tissues with rates of protein synthesis being decreased after only three hours at 50% air saturation (Fig. 4B,C).

Protein degradation

Markers of the ubiquitin proteasome pathway, calpain and autophagy pathways were measured in liver, muscle and heart (Table 1, 2 and 3, respectively). Ubiquitin proteasome pathway markers were unaffected in liver and muscle, but in heart, *Fbxo25* and *UBE2H* transcript levels were decreased at 15% air saturation ($p<0.01$, $n=5$; Table 3). Polyubiquitinated protein levels were unchanged in all tissues (Fig. S1). In the calpain pathway, *calpain7* transcripts levels increased at

15% air saturation in liver and decreased in heart (p=0.004, n=5). *Calpastatin* transcript levels also increased in liver at 50%, 30% and 15% air saturation (p=0.003, n=5), but did not change in muscle and heart. Autophagy-related transcripts, *Cathepsin D* and *LC3B* increased in liver as air saturation decreased (p<0.001, n=5; Table 1). In heart , transcripts levels of *Cathepsin L* (p=0.04, n=5), *Atg4* (p=0.04, n=5), and *Beclin1* (p=0.001, n=5) were lowered at 15% air saturation (Table 3).

Activation of oxygen sensitive signalling pathways

In the mTOR pathway, the phosphorylation levels of AMPKα, 4EBP1 were measured in liver, muscle and heart (Fig. 5). AMPKα phosphorylation increased in liver and heart at 15% air saturation (p<0.001, n=5; Fig. 5A-C). In all three tissues, phosphorylation levels of 4EBP1 decreased at 15% air saturation compared to controls (p<0.001, n=5; Fig. 5D-F). Activation of the unfolded protein response pathway was assessed by measuring eIF2α phosphorylation (Fig. 5G-I) and transcript levels of *eIF2α*, *ATF4* and *DDIT3*. The phosphorylation levels of eIF2α were higher at 15% air saturation in liver and muscle (p<0.001, n=5; Fig. 5G-H). In heart, eIF2α phosphorylation decreased at 50% and 30%, before returning to control levels at 15% (p=0.01, n=5; Fig. 5I). The hypoxia treatments had no effects on *eIF2α* transcripts in all tissues, but levels of *ATF4* transcripts were only affected in heart (p=0.02, n=5) where transcript levels decreased at 15% air saturation (Table 3). *DDIT3* transcripts showed opposite responses in liver and muscle. *DDIT3* transcript levels gradually increased in liver as air saturation decreased (p=0.02, n=5; Table 1), while *DDIT3* transcripts decreased in muscle with decreasing air saturation (p=0.01, n=5; Table 2). No changes occurred for *DDIT3* transcripts in heart (Table 3). Commercial antibodies for HIF-1 working in salmonids are not available, therefore we used the transcripts numbers of gene involved in the pathway. In liver, transcript levels for *HIF1a* (p<0.001, n=5) and its target *VEGF* (p=0.007, n=5) were elevated in fish exposed to 50% air saturation, and this elevation was maintained at 30% and 15% (Table 1). *VHL* transcript numbers in the liver were not significantly affected although they showed a similar trend (p=0.06, n=5) to *VEGF* (Table 1). In muscle, *HIF1a* transcripts remained unchanged, while *VEGF* transcript levels decreased at 30% and 15% air saturation (p<0.001, n=5), and *VHL* increased at 50% and 30% air saturation (p=0.004, n=5; Table 2). In heart, there were no changes for *HIF1a* and *VHL* transcript levels, but *VEGF* transcripts increased at 15% air saturation (p<0.001, n=5; Table 3).

Discussion

Our objectives were to determine whether protein metabolism was deregulated in different tissues of Arctic char during cumulative, graded hypoxia. The fish were exposed to a graded hypoxia protocol with a first step of hypoxia at 50% air saturation for 3 hours. At this concentration, the fish were already in an hypoxic metabolic state, as demonstrated by the elevated plasma and liver lactate concentrations (van Raaij et al., 1996; Via et al., 1997; Wood et al., 2007; Zhou et al., 2005). We should also acknowledge that during each subsequent trial (30% and 15% air saturation) more time was allowed for biochemical responses as well as gene expression to occur, which could bias the comparisons of the hypoxia response at each level. Nevertheless, our study showed that protein metabolism in Arctic char is altered in a tissue-specific fashion during graded hypoxia, which is in accordance with the responses of the three major hypoxia-sensitive pathways (HIF, UPR and mTOR), as observed in mammalian cells.

Protein synthesis

The rate of protein synthesis was highly responsive to graded hypoxia in Arctic char. The effects of hypoxia on the rate of protein synthesis is documented in hypoxia-tolerant fish species (Cassidy et al., 2018; Lewis et al., 2007; Smith et al., 1996; Zhou et al., 2005), but to our knowledge, we report for the first time that it is also the case in hypoxia-sensitive species such as Arctic char. At 50% air saturation, some tissues like the liver and the digestive tract were already responding to hypoxia by decreasing their rate of protein synthesis by ~20% air saturation, while protein synthesis in the heart seemed insensitive to graded hypoxia even at air saturation of 15%. Overall, liver and digestive system showed the most dramatic decreases of protein synthesis rates, reflecting the sensitivity of these tissues to changes in oxygen availability and their triviality for short-term survival. Skeletal muscle comprises over 50% of the fish's body mass, therefore suppressing muscle protein synthesis by half significantly decreases resting metabolic rate. The only tissue that maintained its rate of protein synthesis throughout the graded hypoxia experiment is the heart, contrasting with our previous findings on the hypoxia-tolerant oscar (Cassidy et al., 2018). The heart of most fish, including oscars, receives oxygen from venous blood (Farrell, 2002), therefore when oxygen is limiting, cardiac functions are impaired (Farrell, 2002). In oscars, since energy demand during hypoxia is so low, a decrease in heart function could have little effect on survival.

In the salmonid heart, about 30% of the myocardium is supplemented by a coronary artery (Farrell, 2002), which probably explains how Arctic char's heart maintained protein synthesis during hypoxia. This anabolic state may also be fuelled by the increase in plasma lactate, one of the preferred metabolic substrate of salmonid hearts (Milligan and Farrell, 1991).

Protein degradation

The effects of hypoxia on protein degradation-related markers have scarcely been studied in fish (Cassidy et al., 2018). Our results provide strong evidence that protein degradation plays an important role in the hypoxia response. Markers of the ubiquitin proteasome pathway, autophagy and calpain system showed different trends among tissues. Overall, muscle protein degradation was maintained during hypoxia, supporting the lack of responses measured in the oxygen response pathways. However, liver and heart showed large but opposing effects of hypoxia on protein degradation markers. In mammals, hypoxia is a well-documented inducer of autophagy (Fang et al., 2015; Schaaf et al., 2013), but this is not yet verified in fish. In liver, autophagy was activated during graded hypoxia, as shown by the elevation of *LC3B* transcripts, the hallmark marker of autophagy activation. This increase in autophagy is similar to what's observed in mammals, and likely reflects the liver's sensitivity to hypoxia. Perhaps surprisingly, the ubiquitin proteasome pathway markers were unresponsive to hypoxia in the Arctic char liver, contrasting with a downregulation of proteasome-subunit mRNAs, previously reported in hypoxic three-spine stickleback (Leveelahti et al., 2011). It is likely that this discrepancy results from the different hypoxia protocols the two experiments are using but this issue remains to be further clarified by including a higher number of genes and looking at protein abundance.

In the heart, graded hypoxia was accompanied by an unexpected downregulation of protein degradation markers of all three pathways. Ubiquitin proteasome and calpain markers (*Fbxo25*, *UBE2H* and *Calpain 7*) decreased, suggesting a downregulation of these two pathways. Transcripts from the autophagy pathway also decreased at 15% air saturation, which is opposite to what we observed in Arctic char liver and what is known in mammals (Mazure and Pouysségur, 2010; Wouters and Koritzinsky, 2008). We offer two potential explanations for this. First, decreasing protein degradation might protect the heart's main functions by allocating more energy towards other more vital ones, such as contractions and protein synthesis. It is also possible that

during hypoxia, the Arctic char heart is in an anabolic state supplied by an increase in plasma lactate. This hypothesis is also supported by the maintained rates of protein synthesis in the heart. A decrease in protein degradation during an anabolic state would maximize protein retention and thereby increase heart growth in the event of long-term hypoxia exposure, or during multiple exposures (diel cycling). An enlarged heart could then increase cardiac output , to increase Arctic char's ability to deliver oxygen to tissues (Driedzic et al., 1996; Marques et al., 2008). These results warrant further investigation to understand the role of protein degradation inhibition in the heart during hypoxia.

Hypoxia response pathways

We measured the activation of the three major hypoxia response cellular signalling pathways (HIF, UPR and mTOR) in liver, muscle and heart by looking at the phosphorylation of key proteins involved in each pathway and/or the transcript numbers of genes under their control. These pathways promote energy conservation and enhance survival under low oxygen conditions (Liu et al., 2006). Our results confirm that these pathways are also regulated in hypoxia-sensitive fish, and in a tissue-specific manner.

In liver, the hypoxia response pathways were regulated as documented in mammals (Wouters and Koritzinsky, 2008). First, HIF was activated, and later UPR was activated during the more severe graded hypoxia exposure, while the mTOR pathway was inhibited. The HIF pathway was activated early during hypoxia as shown by the rapid elevation of its target gene, *VEGF* transcripts (Wouters and Koritzinsky, 2008). This might also be supported by the observed increase of *HIF1a* transcripts. Although measuring *HIF1a* transcripts is not directly related to HIF accumulation in tissues, transcript levels increased during hypoxia in several fish species and this has been associated to HIF activation (Heinrichs-Caldas et al., 2019; Rimoldi et al., 2012; Ton et al., 2003). The UPR was activated during severe graded hypoxia, as shown by the accumulation of phosphorylated eIF2α. This is similar to what is observed in oscar livers (Cassidy et al., 2018). The gradual activation of AMPK as the graded hypoxia treatment progresses, eventually translated into an inhibition of the mTOR pathway (shown by the dephosphorylation of 4EBP1). These results are similar to goldfish that increased AMPK activity in the liver during hypoxia (Jibb and Richards, 2008). The dephosphorylation of 4EBP1 results in a depression of cap-dependent

translation consistent with the depression of the rate of protein synthesis we observed (Richter and Sonenberg, 2005). Overall, the hypoxia response pathways were strongly regulated in liver, and in accordance with the large decrease in protein synthesis and increase of autophagy markers. These results suggest that when oxygen decreases and blood becomes hypoxemic, oxygen delivery curtails early in liver.

In muscle, the hypoxia response pathways were regulated differently than in liver. The transcript numbers of *VEGF* decreased as hypoxia progressed which would be consistent with a greater destabilization of HIF in this tissue. Furthermore, the transcript numbers of *VHL*, which is responsible for the selective degradation of HIF (Turcotte et al., 2008), was rapidly elevated during hypoxia. Downregulation of the HIF pathway in muscle during hypoxia is surprising but suggests that muscle vascularization was impeded. To our knowledge, *VEGF* transcripts were never measured in the skeletal muscle of fish during hypoxia. The UPR was activated during the most severe hypoxia treatment in muscle, and mTOR was inhibited (decreased 4EBP1 phosphorylation), which is consistent with the decreased rates of protein synthesis in muscle. The regulation of protein synthesis *via* signalling pathways is important to reduce energy expenditure and the load of proteins in the ER, even in muscle, which otherwise appeared to have low sensitivity to hypoxia.

Out of the three examined tissues, the heart was the least responsive to hypoxia. There was a late activation of the HIF pathway, as *VEGF* transcripts increased at 15% air saturation and the UPR pathway was not activated. Similarly, AMPK and mTOR pathways responded as if the heart became anabolic during intermediate oxygen concentrations. The pattern of activation of these oxygen responsive signalling pathways indicates that the heart is one of the last tissues to become hypoxic, probably as a result of preferential oxygen supply via the coronary artery (Gamperl et al., 1995). The apparent anabolic state of the heart during hypoxia is metabolically fuelled by the circulating muscle-derived lactate as suggested by Lanctin et al. (1980) and Milligan and Farrell (1991).

Conclusion

We show that despite being a hypoxia intolerant species, Arctic char demonstrate considerable ability to alter protein metabolism, which could be under the control of hypoxia

responsive cellular signalling pathways (HIF, UPR and mTOR). The activation pattern of these pathways and the cellular processes that are under their control varies greatly among tissues, sometimes even going in opposite direction. This study provides new insights on the effects of hypoxia on protein metabolism. The adjustments of these cellular processes probably all contribute in shifting the fish phenotype into a more hypoxia-tolerant one. Here we measure the response of protein metabolism to a single and cumulative, graded hypoxia event in fish that were naïve to hypoxia. Our results warrant studying these adjustments in fish exposed to long-term and diel cycling hypoxia.

Acknowledgments

The authors are grateful to André Dumas and Claude Pelletier at the Coastal Zones Research Institute (Shippagan, NB, Canada) for providing the fish.

Competing interests

The authors declare no competing or financial interests.

Author contributions

Conceptualization: A.A.C., and S.G.L.; Methodology: A.A.C.; Formal analysis: A.A.C.; Writing original draft: A.A.C.; Writing - review & editing: A.A.C., and S.G.L.; Funding acquisition: S.G.L.

Funding

A.A.C. was supported by a Natural Sciences and Engineering Research Council of Canada (NSERC) Postgraduate Scholarship-Doctoral Program (PGSD). S.G.L. was supported by grants from NSERC [435638-2013].

References

Baptista, R. B., Souza-Castro, N. and Almeida-Val, V. M. F. (2016). Acute hypoxia up-regulates HIF-1α and VEGF mRNA levels in Amazon hypoxia-tolerant Oscar (*Astronotus ocellatus*). *Fish Physiol. Biochem.* **42**, 1307–1318.

Boutilier, R. G. (2001). Mechanisms of cell survival in hypoxia and hypothermia. *J. Exp. Biol.* **204**, 3171–3181.

Bradford, M. M. (1976). A rapid and sensitive method for the quantitation of microgram quantities of protein utilizing the principle of protein-dye binding. *Anal. Biochem.* **72**, 248–254.

Brandt, R. B., Siegel, S. A., Waters, M. G. and Bloch, M. H. (1980). Spectrophotometric assay for D-(−)-lactate in plasma. *Anal. Biochem.* **102**, 39–46.

Bustin, S. A., Benes, V., Garson, J. A., Hellemans, J., Huggett, J., Kubista, M., Mueller, R., Nolan, T., Pfaffl, M. W., Shipley, G. L., et al. (2009). The MIQE Guidelines: Minimum Information for Publication of Quantitative Real-Time PCR Experiments. *Clin. Chem.* **55**, 611.

Cam, H. and Houghton, P. J. (2011). Regulation of mammalian target of rapamycin complex 1 (mTORC1) by hypoxia: causes and consequences. *Target. Oncol.* **6**, 95–102.

Cassidy, A. A., Saulnier, R. J. and Lamarre, S. G. (2016). Adjustments of protein metabolism in fasting Arctic charr, *Salvelinus alpinus*. *PLOS ONE* **11**, e0153364.

Cassidy, A. A., Driedzic, W. R., Campos, D., Heinrichs-Caldas, W., Almeida-Val, V. M. F., Val, A. L. and Lamarre, S. G. (2018). Protein synthesis is lowered by 4EBP1 and eIF2-α signaling while protein degradation may be maintained in fasting, hypoxic Amazonian cichlids *Astronotus ocellatus*. *J. Exp. Biol.* **221**,.

Ciechanover, A. (2012). Intracellular protein degradation: from a vague idea through the lysosome and the ubiquitin-proteasome system and onto human diseases and drug targeting. *Neurodegener. Dis.* **10**, 7–22.

Ciechanover, A., Finley, D. and Varshavsky, A. (1984). The ubiquitin- mediated proteolytic pathway and mechanisms of energy- dependent intracellular protein degradation. *J. Cell. Biochem.* **24**, 27–53.

Cui, W., Zhou, J., Dehne, N. and Brüne, B. (2015). Hypoxia induces calpain activity and degrades SMAD2 to attenuate TGFβ signaling in macrophages. *Cell Biosci.* **5**, 36.

Driedzic, W. R., Bailey, J. R. and Sephton, D. H. (1996). Cardiac adaptations to low temperature in non-polar teleost fish. *J. Exp. Zool.* **275**, 186–195.

Fader, C. M., Aguilera, M. O. and Colombo, M. I. (2015). Autophagy response: manipulating the mTOR-controlled machinery by amino acids and pathogens. *Amino Acids* **47**, 2101–2112.

Fang, Y., Tan, J. and Zhang, Q. (2015). Signaling pathways and mechanisms of hypoxia-induced autophagy in the animal cells. *Cell Biol. Int.* **39**, 891–898.

Farrell, A. P. (2002). Cardiorespiratory performance in salmonids during exercise at high temperature: insights into cardiovascular design limitations in fishes. *Comp. Biochem. Physiol. A. Mol. Integr. Physiol.* **132**, 797–810.

Farrell, A. P. and Richards, J. G. (2009). Defining hypoxia: an integrative synthesis of the responses of fish to hypoxia. In *Hypoxia* (ed. Jeffrey G. Richards, A. P. F.) and Brauner, C. J.), pp. 487–503. Academic Press.

Gamperl, A. K., Axelsson, M. and Farrell, A. P. (1995). Effects of swimming and environmental hypoxia on coronary blood flow in rainbow trout. *Am. J. Physiol.-Regul. Integr. Comp. Physiol.* **269**, R1258–R1266.

Garlick, P. J., McNurlan, M. A. and Preedy, V. R. (1980). A rapid and convenient technique for measuring the rate of protein synthesis in tissues by injection of [3H]phenylalanine. *Biochem. J.* **192**, 719–723.

Glickman, M. H. and Ciechanover, A. (2002). The Ubiquitin-Proteasome Proteolytic Pathway: Destruction for the Sake of Construction. *Physiol. Rev.* **82**, 373–428.

Goll, D. E., Thompson, V. F., Li, H., Wei, W. and Cong, J. (2003). The Calpain System. *Physiol. Rev.* **83**, 731.

Gozal, D., Row, B., Kheirandish, L., Liu, R., Guo, S. Z., Qiang, F. and Brittian, K. R. (2003). Increased susceptibility to intermittent hypoxia in aging rats: changes in proteasomal activity, neuronal apoptosis and spatial function. *J. Neurochem.* **86**, 1545–1552.

Gürtler, A., Kunz, N., Gomolka, M., Hornhardt, S., Friedl, A. A., McDonald, K., Kohn, J. E. and Posch, A. (2013). Stain-Free technology as a normalization tool in Western blot analysis. *Anal. Biochem.* **433**, 105–111.

Hay, N. and Sonenberg, N. (2004). Upstream and downstream of mTOR. *Genes Dev.* **18**, 1926–1945.

Heinrichs-Caldas, W., Campos, D. F., Paula-Silva, M. N. and Almeida-Val, V. M. F. (2019). Oxygen-dependent distinct expression of hif-1α gene in aerobic and anaerobic tissues of the Amazon Oscar, *Astronotus crassipinnis*. *Comp. Biochem. Physiol. B Biochem. Mol. Biol.* **227**, 31–38.

Jibb, L. A. and Richards, J. G. (2008). AMP-activated protein kinase activity during metabolic rate depression in the hypoxic goldfish, *Carassius auratus*. *J. Exp. Biol.* **211**, 3111.

Johnston, I. A., Bower, N. I. and Macqueen, D. J. (2011). Growth and the regulation of myotomal muscle mass in teleost fish. *J. Exp. Biol.* **214**, 1617–1628.

Jones, I. D., Winfield, I. J. and Carse, F. (2008). Assessment of long- term changes in habitat availability for Arctic charr (*Salvelinus alpinus*) in a temperate lake using oxygen profiles and hydroacoustic surveys. *Freshw. Biol.* **53**, 393–402.

Koressaar, T. and Remm, M. (2007). Enhancements and modifications of primer design program Primer3. *Bioinformatics* **23**, 1289–1291.

Kumar, S., Stecher, G. and Tamura, K. (2016). MEGA7: Molecular Evolutionary Genetics Analysis Version 7.0 for Bigger Datasets. *Mol. Biol. Evol.* **33**, 1870–1874.

Lamarre, S. G., Saulnier, R. J., Blier, P. U. and Driedzic, W. R. (2015). A rapid and convenient method for measuring the fractional rate of protein synthesis in ectothermic animal tissues using a stable isotope tracer. *Comp. Biochem. Physiol. B Biochem. Mol. Biol.* **182**, 1–5.

Lanctin, H. P., McMorran, L. E. and Driedzic, W. R. (1980). Rates of glucose and lactate oxidation by the perfused isolated trout (*Salvelinus fontinalis*) heart. *Can. J. Zool.* **58**, 1708–1711.

Leveelahti, L., Leskinen, P., Leder, E. H., Waser, W. and Nikinmaa, M. (2011). Responses of threespine stickleback (*Gasterosteus aculeatus*, L) transcriptome to hypoxia. *Comp. Biochem. Physiol. Part D Genomics Proteomics* **6**, 370–381.

Lewis, J. M., Costa, I., Val, A. L., Almeida-Val, V. M. F., Gamperl, A. K. and Driedzic, W. R. (2007). Responses to hypoxia and recovery: repayment of oxygen debt is not associated with compensatory protein synthesis in the Amazonian cichlid, *Astronotus ocellatus*. *J. Exp. Biol.* **210**, 1935–1943.

Liu, L., Cash, T. P., Jones, R. G., Keith, B., Thompson, C. B. and Simon, M. C. (2006). Hypoxia-induced energy stress regulates mRNA translation and cell growth. *Mol. Cell* **21**, 521–531.

Marques, I. J., Leito, J. T. D., Spaink, H. P., Testerink, J., Jaspers, R. T., Witte, F., van den Berg, S. and Bagowski, C. P. (2008). Transcriptome analysis of the response to chronic constant hypoxia in zebrafish hearts. *J. Comp. Physiol. B* **178**, 77–92.

Mazurais, D., Ferraresso, S., Gatta, P. P., Desbruyères, E., Severe, A., Corporeau, C., Claireaux, G., Bargelloni, L. and Zambonino-Infante, J.-L. (2014). Identification of hypoxia-regulated genes in the liver of common sole (*Solea solea*) fed different dietary lipid contents. *Mar. Biotechnol.* **16**, 277–288.

Mazure, N. M. and Pouysségur, J. (2010). Hypoxia-induced autophagy: cell death or cell survival? *Cell Regul.* **22**, 177–180.

Milligan, C. L. and Farrell, A. P. (1991). Lactate utilization by an *In Situ* perfused trout heart: Effects of workload and blockers of lactate transport. *J. Exp. Biol.* **155**, 357.

Mungai, P. T., Waypa, G. B., Jairaman, A., Prakriya, M., Dokic, D., Ball, M. K. and Schumacker, P. T. (2011). Hypoxia triggers AMPK activation through reactive oxygen

species-mediated activation of calcium release-activated calcium channels. *Mol. Cell. Biol.* **31**, 3531–3545.

Nanduri, J., Wang, N., Yuan, G., Khan, S. A., Souvannakitti, D., Peng, Y.-J., Kumar, G. K., Garcia, J. A. and Prabhakar, N. R. (2009). Intermittent hypoxia degrades HIF-2α via calpains resulting in oxidative stress: Implications for recurrent apnea-induced morbidities. *Proc. Natl. Acad. Sci.* **106**, 1199.

Neufeld, G., Cohen, T., Gengrinovitch, S. and Poltorak, Z. (1999). Vascular endothelial growth factor (VEGF) and its receptors. *FASEB J.* **13**, 9–22.

Papandreou, I., Lim, A. L., Laderoute, K. and Denko, N. C. (2008). Hypoxia signals autophagy in tumor cells via AMPK activity, independent of HIF-1, BNIP3, and BNIP3L. *Cell Death Differ.* **15**, 1572.

Pfaffl, M. W. (2001). A new mathematical model for relative quantification in real-time RT-PCR. *Nucleic Acids Res.* **29**, e45.

Richards, J. G. (2010). Physiological, behavioral and biochemical adaptations of intertidal fishes to hypoxia. *J. Exp. Biol.* **214**, 191–199.

Richter, J. D. and Sonenberg, N. (2005). Regulation of cap-dependent translation by eIF4E inhibitory proteins. *Nature* **433**, 477–480.

Rimoldi, S., Terova, G., Ceccuzzi, P., Marelli, S., Antonini, M. and Saroglia, M. (2012). HIF-1α mRNA levels in Eurasian perch (*Perca fluviatilis*) exposed to acute and chronic hypoxia. *Mol. Biol. Rep.* **39**, 4009–4015.

Ron, D. and Walter, P. (2007). Signal integration in the endoplasmic reticulum unfolded protein response. *Nat Rev Mol Cell Biol* **8**, 519–529.

Schaaf, M. B. E., Cojocari, D., Keulers, T. G., Jutten, B., Starmans, M. H., de Jong, M. C., Begg, A. C., Savelkouls, K. G. M., Bussink, J., Vooijs, M., et al. (2013). The autophagy associated gene, ULK1, promotes tolerance to chronic and acute hypoxia. *Radiother. Oncol.* **108**, 529–534.

Schofield, C. J. and Ratcliffe, P. J. (2004). Oxygen sensing by HIF hydroxylases. *Nat. Rev. Mol. Cell Biol.* **5**, 343.

Shen, R.-J., Jiang, X.-Y., Pu, J.-W. and Zou, S.-M. (2010). HIF-1α and -2α genes in a hypoxia-sensitive teleost species Megalobrama amblycephala: cDNA cloning, expression and different responses to hypoxia. *Comp. Biochem. Physiol. B Biochem. Mol. Biol.* **157**, 273–280.

Smith, R. W., Houlihan, D. F., Nilsson, G. E. and Brechin, J. G. (1996). Tissue-specific changes in protein synthesis rates in vivo during anoxia in crucian carp. *Am. J. Physiol. - Regul. Integr. Comp. Physiol.* **271**, R897–R904.

Sun, S., Wu, Y., Fu, H., Yang, M., Ge, X., Zhu, J., Xuan, F. and Wu, X. (2019). Evaluating expression of autophagy-related genes in oriental river prawn Macrobrachium nipponense as potential biomarkers for hypoxia exposure. *Ecotoxicol. Environ. Saf.* **171**, 484–492.

Ton, C., Stamatiou, D. and Liew, C.-C. (2003). Gene expression profile of zebrafish exposed to hypoxia during development. *Physiol. Genomics* **13**, 97–106.

Turcotte, S., Chan, D. A., Sutphin, P. D., Hay, M. P., Denny, W. A. and Giaccia, A. J. (2008). A molecule targeting VHL-deficient renal cell carcinoma that induces autophagy. *Cancer Cell* **14**, 90–102.

Untergasser, A., Cutcutache, I., Koressaar, T., Ye, J., Faircloth, B. C., Remm, M. and Rozen, S. G. (2012). Primer3—new capabilities and interfaces. *Nucleic Acids Res.* **40**, e115–e115.

van Raaij, M. T. M., Pit, D. S. S., Balm, P. H. M., Steffens, A. B. and van den Thillart, G. E. E. J. M. (1996). Behavioral strategy and the physiological stress response in rainbow trout exposed to severe hypoxia. *Horm. Behav.* **30**, 85–92.

Vandesompele, J., De Preter, K., Pattyn, F., Poppe, B., Van Roy, N., De Paepe, A. and Speleman, F. (2002). Accurate normalization of real-time quantitative RT-PCR data by geometric averaging of multiple internal control genes. *Genome Biol.* **3**, research0034.1.

Via, J. D., van den Thillart, G., Cattani, O. and Cortesi, P. (1997). Environmental versus functional hypoxia/anoxia in sole *Solea solea*: the lactate paradox revisited. *Mar. Ecol. Prog. Ser.* **154**, 79–90.

Williams, K. J., Cassidy, A. A., Verhille, C. E., Lamarre, S. G. and MacCormack, T. J. (2019). Diel cycling hypoxia enhances hypoxia tolerance in rainbow trout (*Oncorhynchus mykiss*): evidence of physiological and metabolic plasticity. *J. Exp. Biol.* **222**, jeb206045.

Wood, C. M., Kajimura, M., Sloman, K. A., Scott, G. R., Walsh, P. J., Almeida-Val, V. M. F. and Val, A. L. (2007). Rapid regulation of Na^+ fluxes and ammonia excretion in response to acute environmental hypoxia in the Amazonian oscar, *Astronotus ocellatus*. *Am. J. Physiol. - Regul. Integr. Comp. Physiol.* **292**, R2048–R2058.

Wouters, B. G. and Koritzinsky, M. (2008). Hypoxia signalling through mTOR and the unfolded protein response in cancer. *Nat Rev Cancer* **8**, 851–864.

Zhang, K. and Kaufman, R. J. (2006). Protein folding in the endoplasmic reticulum and the Unfolded Protein Response. In *Molecular Chaperones in Health and Disease* (ed. Starke, K.) and Gaestel, M.), pp. 69–91. Berlin, Heidelberg: Springer Berlin Heidelberg.

Zhou, B. S., Wu, R. S., Randall, D. J., Lam, P. K. S., Ip, Y. K. and Chew, S. (2005). Metabolic adjustments in the common carp during prolonged hypoxia. *J. Fish Biol.* **57**, 1160–1171.

Tables

Table 1. Relative transcript levels of mRNAs in liver of Arctic char exposed to 100%, 50%, 30% and 15% air saturation. Transcript levels are normalized with *e1fα*, *α-tubulin* and *rs11*. All data are relative to control levels and expressed as mean ± s.e.m. Lower case letters indicate significant differences ($p < 0.05$) between air saturation levels.

		Liver relative transcript levels (mean ± s.e.m.)			
Pathway	**Name**	**100%**	**50%**	**30%**	**15%**
HIF	*HIF1a*	1.00 ± 0.08^{a}	1.88 ± 0.10^{b}	1.67 ± 0.12^{b}	1.78 ± 0.10^{b}
	VEGF	1.00 ± 0.12^{a}	1.80 ± 0.21^{b}	2.56 ± 0.86^{b}	1.90 ± 0.15^{b}
	VHL	1.00 ± 0.09	1.35 ± 0.09	1.35 ± 0.09	1.19 ± 0.08
UPR	*eIF2α*	1.00 ± 0.08	1.30 ± 0.08	1.03 ± 0.06	1.13 ± 0.12
	ATF4	1.00 ± 0.11	1.10 ± 0.17	1.12 ± 0.11	1.05 ± 0.05
	DDIT3	1.00 ± 0.09^{a}	1.59 ± 0.37^{ab}	2.77 ± 0.58^{b}	2.29 ± 0.71^{ab}
Proteasome	*Fbxo25*	1.00 ± 0.10	1.30 ± 0.17	1.14 ± 0.09	1.14 ± 0.07
Calpains	*Calpain 7*	1.00 ± 0.04^{ab}	1.05 ± 0.10^{ab}	0.87 ± 0.04^{a}	1.33 ± 0.10^{b}
	Calpain small subunit1	1.00 ± 0.10	1.18 ± 0.10	1.24 ± 0.14	1.16 ± 0.09
	Calpastatin	1.00 ± 0.08^{a}	1.43 ± 0.08^{b}	1.61 ± 0.26^{b}	1.46 ± 0.07^{b}
Autophagy	Cathepsin D	1.00 ± 0.12^{a}	1.45 ± 0.08^{b}	1.35 ± 0.09^{ab}	1.36 ± 0.13^{ab}
	Cathepsin L	1.00 ± 0.11	1.06 ± 0.17	1.03 ± 0.10	1.302 ± 0.09
	Atg4	1.00 ± 0.09	0.81 ± 0.12	0.88 ± 0.08	0.84 ± 0.05
	Atg5	1.00 ± 0.02^{ab}	1.15 ± 0.04^{a}	0.95 ± 0.05^{b}	1.09 ± 0.05^{ab}
	Beclin1	1.00 ± 0.09	1.26 ± 0.13	1.11 ± 0.07	1.22 ± 0.15
	LC3A	1.00 ± 0.22	1.29 ± 0.07	1.29 ± 0.10	1.48 ± 0.11
	LC3B	1.00 ± 0.08^{a}	2.30 ± 0.26^{b}	2.82 ± 0.40^{b}	2.72 ± 0.17^{b}

Table 2. Relative transcript levels of mRNAs in muscle of Arctic char exposed to 100%, 50%, 30% and 15% air saturation. Transcript levels are normalized with *e1fα*, *β-actin* and *rs11*. All data are relative to control levels and expressed as mean ± s.e.m. Lower case letters indicate significant differences ($p < 0.05$) between air saturation levels.

		Muscle relative transcript levels (mean ± s.e.m.)			
Pathway	**Name**	**100%**	**50%**	**30%**	**15%**
HIF	*HIF1a*	1.00 ± 0.09	0.76 ± 0.06	0.80 ± 0.06	0.96 ± 0.18
	VEGF	1.00 ± 0.12^{a}	0.82 ± 0.08^{a}	0.51 ± 0.03^{b}	0.45 ± 0.02^{b}
	VHL	1.00 ± 0.42^{a}	2.55 ± 0.19^{b}	2.95 ± 0.30^{b}	2.07 ± 0.32^{ab}
UPR	*eIF2α*	1.00 ± 0.11	0.97 ± 0.08	0.90 ± 0.04	0.81 ± 0.02
	ATF4	1.00 ± 0.1	0.93 ± 0.10	0.92 ± 0.05	0.93 ± 0.15
	DDIT3	1.00 ± 0.12^{a}	0.86 ± 0.10^{a}	0.76 ± 0.08^{ab}	0.53 ± 0.04^{b}
Proteasome	*Mafbx*	1.00 ± 0.22	0.67 ± 0.12	1.18 ± 0.21	1.43 ± 0.39
	Murf1	1.00 ± 0.26	1.85 ± 0.43	2.34 ± 0.69	1.38 ± 0.31
	Fbxo25	1.00 ± 0.16	0.76 ± 0.03	0.72 ± 0.08	0.67 ± 0.08
	UBE2H	1.00 ± 0.23	0.97 ± 0.05	1.09 ± 0.06	1.08 ± 0.13
Calpains	*Calpain 7*	1.00 ± 0.11	0.72 ± 0.06	0.72 ± 0.10	0.71 ± 0.07
	Calpain small subunit1	1.00 ± 0.22	0.89 ± 0.09	1.06 ± 0.17	0.85 ± 0.06
	Calpastatin	1.00 ± 0.11	1.3 ± 0.35	1.1 ± 0.21	1.21 ± 0.19
Autophagy	*Cathepsin D*	1.00 ± 0.12	1.13 ± 0.10	1.16 ± 0.16	1.23 ± 0.18
	Cathepsin L	1.00 ± 0.16^{a}	0.82 ± 0.04^{a}	0.44 ± 0.08^{b}	0.46 ± 0.05^{b}
	Atg4	1.00 ± 0.20	1.13 ± 0.14	1.18 ± 0.22	0.80 ± 0.18
	Atg5	1..00 ± 0.14	0.81 ± 0.06	0.88 ± 0.05	0.90 ± 0.07
	Beclin1	1.00 ± 0.23	0.89 ± 0.11	1.13 ± 0.20	0.76 ± 0.16
	LC3A	1.00 ± 0.08	1.08 ± 0.06	1.17 ± 0.06	1.25 ± 0.11
	LC3B	1.00 ± 0.13	0.92 ± 0.08	0.84 ± 0.07	0.79 ± 0.08

Table 3. Relative transcript levels of mRNAs in heart of Arctic char exposed to 100%, 50%, 30% and 15% air saturation. Transcript levels are normalized with *e1fα*, *β-actin* and *α-tubulin*. All data are relative to control levels and expressed as mean ± s.e.m. Lower case letters indicate significant differences ($p < 0.05$) between air saturation levels.

		Heart relative transcript levels (mean ± s.e.m.)			
Pathway	**Name**	**100%**	**50%**	**30%**	**15%**
HIF	*HIF1a*	1.00 ± 0.12	1.05 ± 0.14	1.21 ± 0.34	1.09 ± 0.12
	VEGF	1.00 ± 0.13^{a}	0.87 ± 0.11^{a}	0.94 ± 0.11^{a}	1.99 ± 0.20^{b}
	VHL	1.00 ± 0.10	1.07 ± 0.11	1.00 ± 0.10	0.81 ± 0.06
UPR	*eIF2α*	1.00 ± 0.08	0.89 ± 0.07	0.88 ± 0.04	0.95 ± 0.04
	ATF4	1.00 ± 0.08^{a}	0.80 ± 0.07^{ab}	0.83 ± 0.05^{ab}	0.69 ± 0.03^{b}
	DDIT3	1.00 ± 0.17	1.06 ± 0.16	1.06 ± 0.10	0.87 ± 0.10
Proteasome	*Fbxo25*	1.00 ± 0.09^{a}	0.93 ± 0.17^{a}	0.73 ± 0.05^{ab}	0.51 ± 0.04^{b}
	UBE2H	1.00 ± 0.14^{a}	0.84 ± 0.13^{a}	0.64 ± 0.05^{ab}	0.54 ± 0.03^{b}
Calpains	*Calpain 7*	1.00 ± 0.06^{a}	0.80 ± 0.10^{ab}	0.65 ± 0.05^{b}	0.61 ± 0.03^{b}
	Calpain small subunit1	1.00 ± 1.6	1.24 ± 0.11	1.24 ± 0.14	0.93 ± 0.08
	Calpastatin	1.00 ± 0.12	1.31 ± 0.35	1.14 ± 021	1.21 ± 0.19
Autophagy	*Cathepsin D*	1.00 ± 0.09	0.94 ± 0.14	0.92 ± 0.04	0.9 ± 0.05
	Cathepsin L	1.00 ± 0.13^{a}	0.78 ± 0.09^{ab}	0.71 ± 0.08^{ab}	0.62 ± 0.04^{b}
	Atg4	1.00 ± 0.07^{ab}	1.11 ± 0.10^{a}	1.05 ± 0.15^{ab}	0.74 ± 0.09^{b}
	Atg5	1.00 ± 0.07	0.92 ± 0.07	0.76 ± 0.09	0.74 ± 0.04
	Beclin1	1.00 ± 0.04^{a}	0.98 ± 0.11^{a}	1.05 ± 0.12^{a}	0.63 ± 0.03^{b}
	LC3A	1.00 ± 0.08	1.19 ± 0.132	1.17 ± 0.12	1.22 ± 0.04
	LC3B	1.00 ± 0.03	0.92 ± 0.08	0.87 ± 0.10	0.79 ± 0.06

Figures

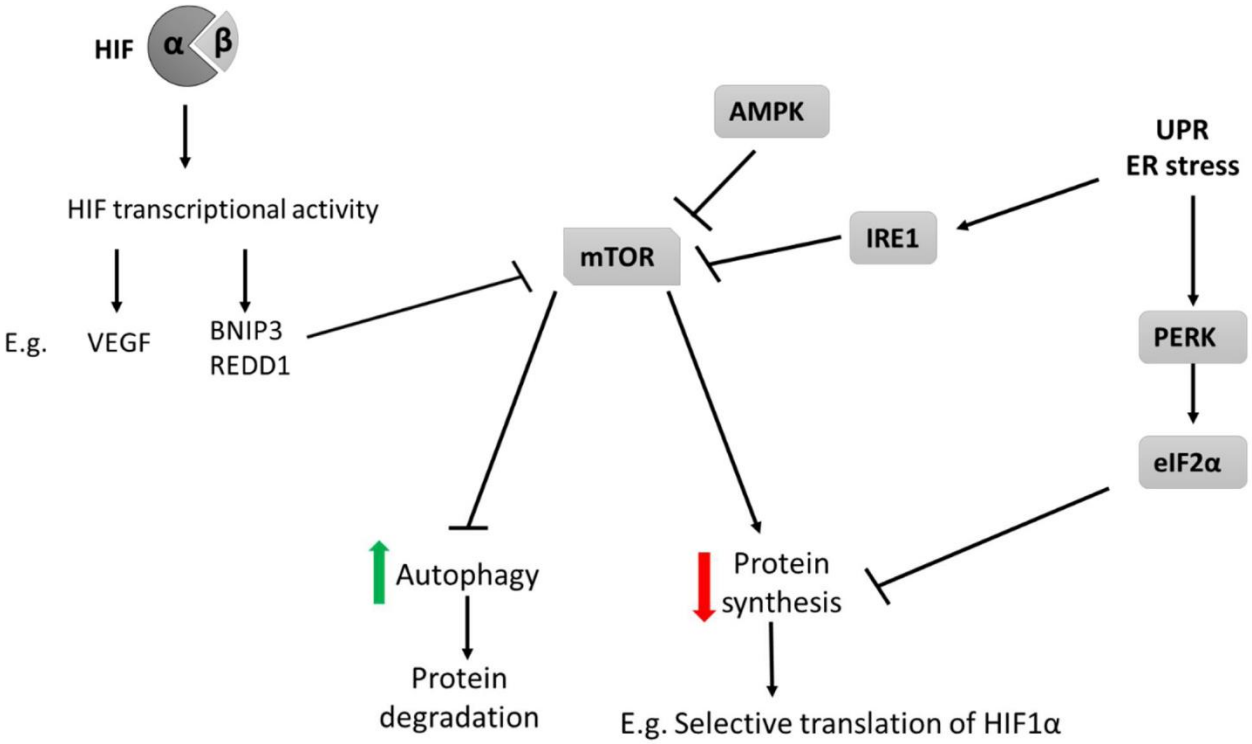

Figure 1. Summary of the three major hypoxia response pathways in mammals. During hypoxia, the hypoxia inducible factor (HIF) pathway is activated when HIFα is allowed to accumulate in cells and forms a complex with HIFβ. This complex than activates the transcription of several target genes in the hypoxia response, including VEGF, BNIP3 and RED11. mTOR is inhibited during hypoxia by several pathways, including AMPK, which results in a decrease in protein synthesis and increase in autophagy. The unfolded protein response (UPR) is also activated because of increased endoplasmic reticulum stress caused by hypoxia. This activates PERK, which phosphorylates eIF2α downstream to inhibit global translation initiation. There is also significant cross talk between the pathways, where mTOR can selectively synthesise HIF proteins and HIF, through BNIP3 and REDD1 can inhibit mTOR. Activation of mTOR and protein synthesis can

exacerbate ER stress, while the UPR can inhibit mTOR through the inhibition of IRS1, a positive regulator of mTOR. This information is summarized from for mammalian tumours (Wouters and Koritzinsky, 2008).

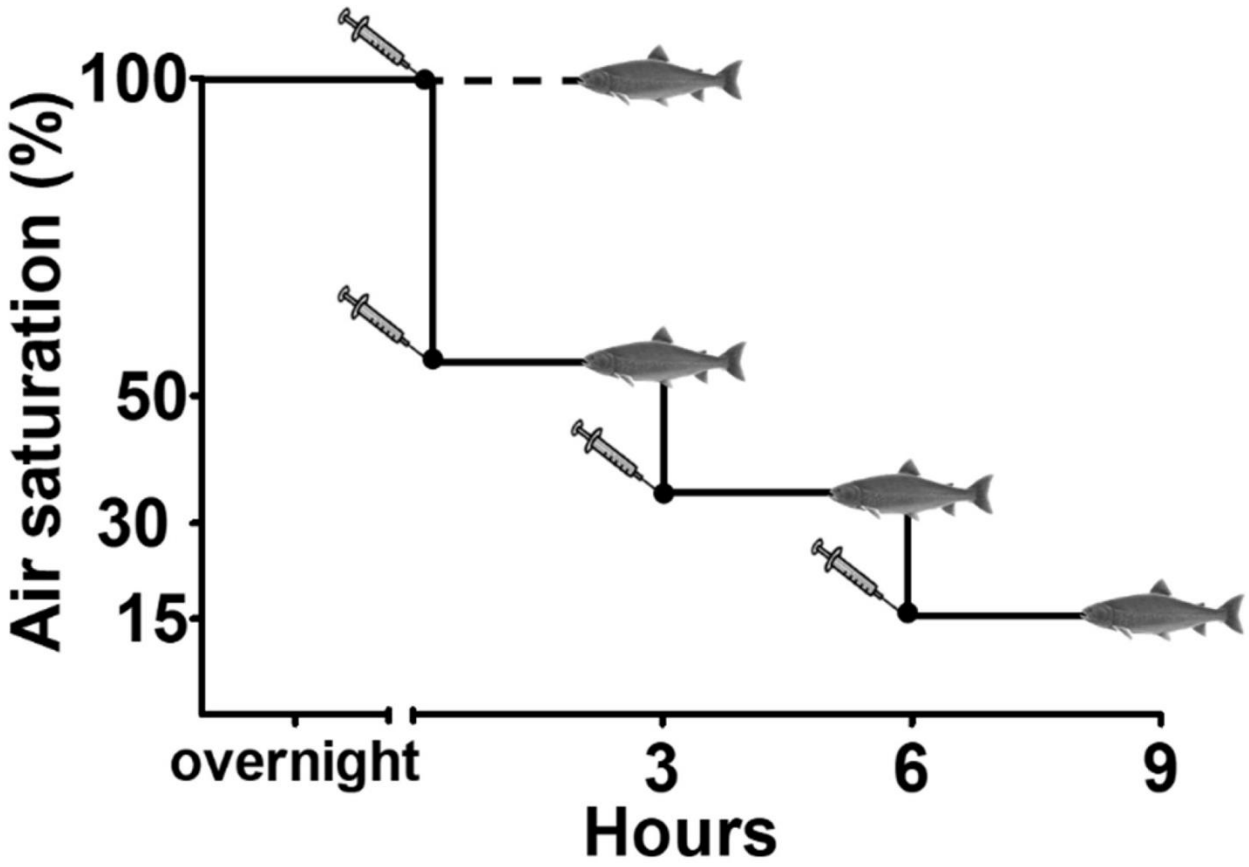

Figure 2. Arctic char were exposed to a stepwise decrease in air saturation before being sampled at (100%, 50%, 30% or 15% air saturation). Using a flooding dose technique, fish were injected with deuterated phenylalanine 3 hours prior to sampling, to measure fractional rates of protein synthesis.

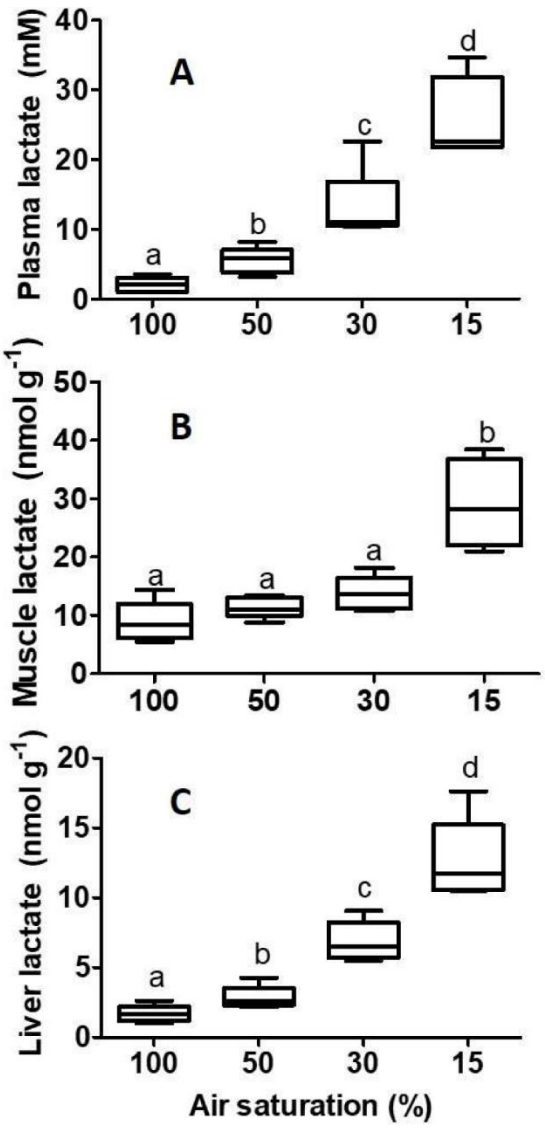

Figure 3. A) Plasma, B) muscle and C) liver lactate (mM) concentration in Arctic char exposed to varying levels of air saturation. Data are expressed as mean ± s.e.m. Lower case letters indicate significant differences ($p < 0.05$) between air saturation levels.

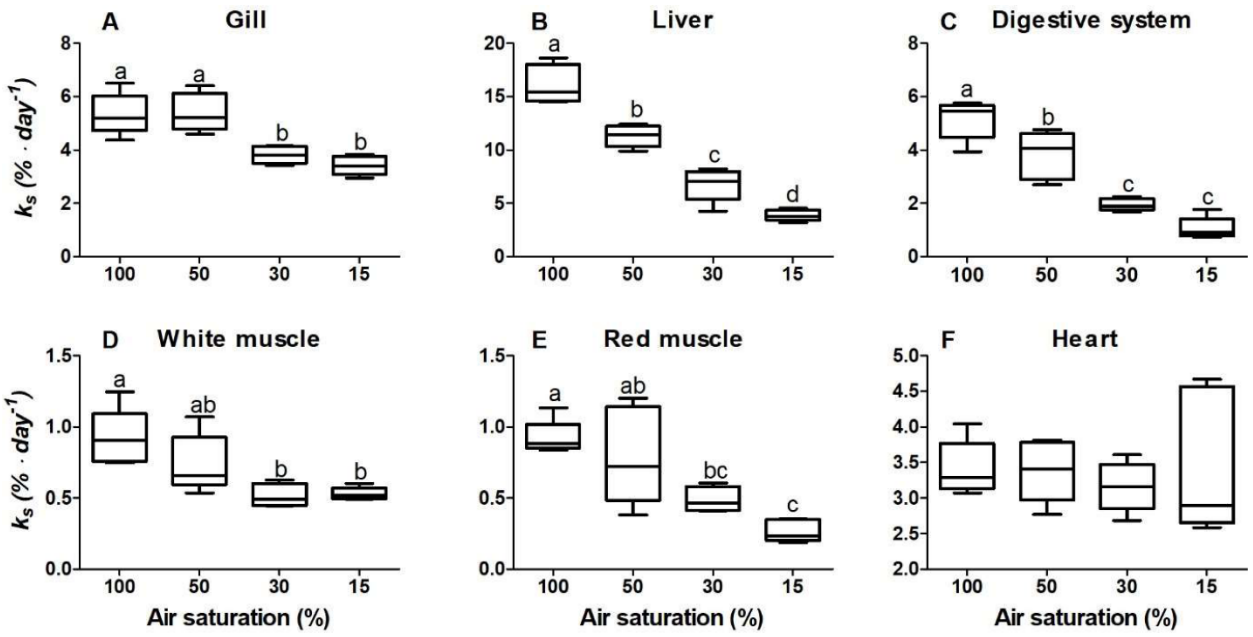

Figure 4. Fractional rates of protein synthesis (k_s %·day^{-1}) of A) gill, B) liver, C) digestive system D) white muscle, E) red muscle and F) heart after exposure to varying levels of air saturation. Values are expressed as mean ± s.e.m. Lower case letters indicate significant differences ($p < 0.05$) between air saturation levels

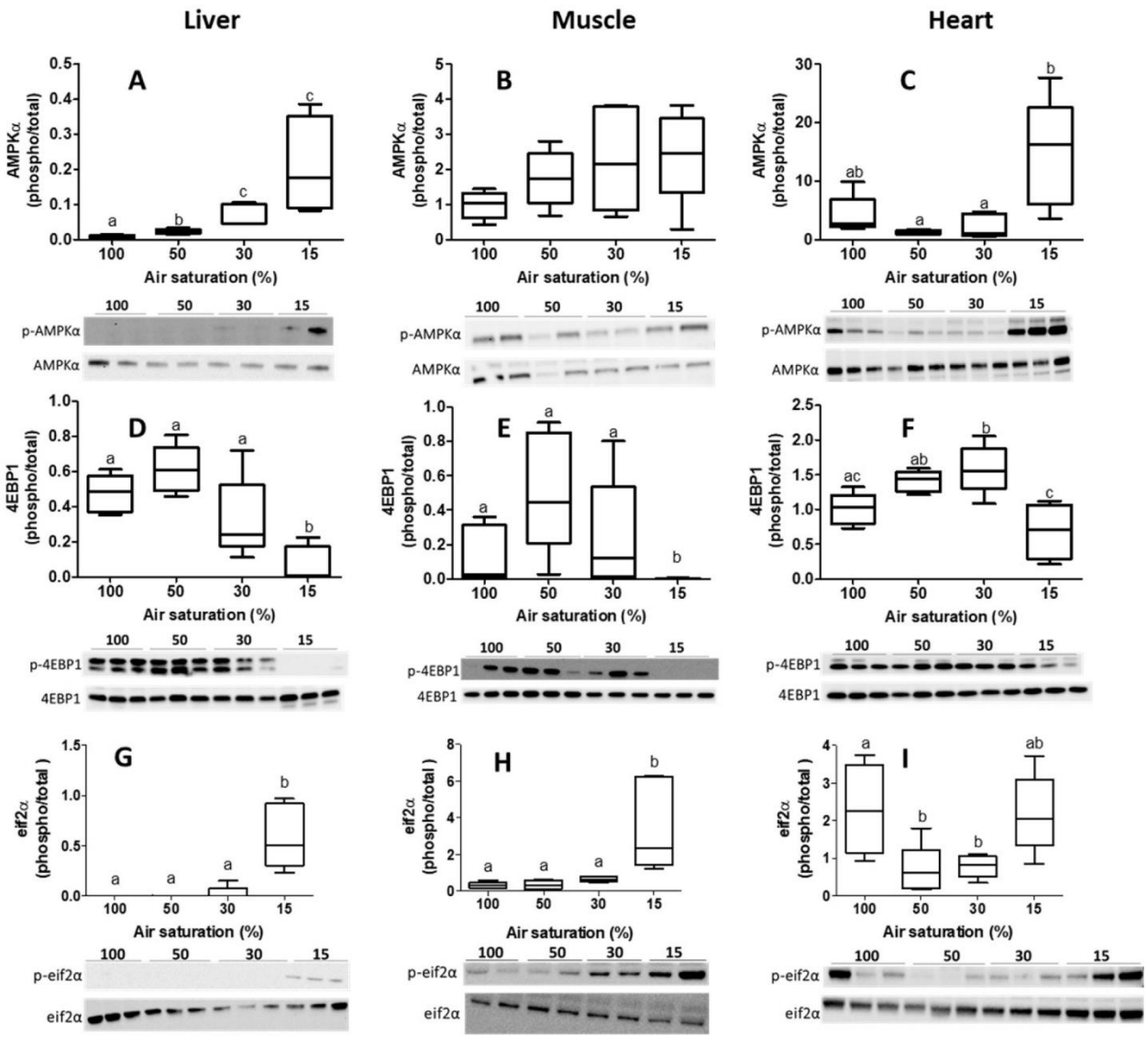

Figure 5. Phosphorylation levels of proteins involved in the hypoxia response pathways. AMPKα is shown in A) liver, B) muscle, and C) heart. 4EBP1 is shown in D) liver, E) muscle and F) heart. eif2α is shown in G) liver, H) muscle and I) heart. Protein levels are normalized to stain-free gel band volumes. Values are expressed as mean ± s.e.m. Lower case letters indicate significant differences ($p < 0.05$) between air saturation levels.

Supplementary information

Table S1. Primer sequences and efficiency (E) in Arctic char skeletal muscle, liver and heart.

Primer		Sequence	Acc. No.	BP	Muscle E (%)	Liver E (%)	Heart E (%)
ATF4	Fwd	5'-AGATGGCACAGAACAAGACG-3'	NM_001140101.1	143	104	95	102
	Rev	5'-GAGTCTGCTTTCTCCGCAAG-3'					
ATG5	Fwd	5'-AGAGCGTGACTTGCTCCACT-3'	NM_001173812.1	109	97	99	110
	Rev	5'-GTCGTTGATGACCTGGCTCT-3'					
ATG4	Fwd	5'- TTGAAGACTTGCCTGACACC-3'	NM_001141602.2	98	107	104	99
	Rev	5'-CGAGTGAACGTCTGATAGGAGT-3'					
α-tubulin	Fwd	5'- CTGACTGTGCCTTCATGGTG-3'	NM_001141467.2	119	99	103	99
	Rev	5'-GGAGGAGACGATCTGACCAA-3'					
β-actin	Fwd	5'-GACGCGACCTCACAGACTAC-3'	NM_001123525.1	79	105	98	109
	Rev	5'-GTGCCCATCTCCTGCTCAAA-3'					
Beclin1	Fwd	5'-GCCTGAAGAAGACCAACGTC-3'	NM_001139818.1	86	107	105	-----
	Rev	5'-GCCCAGACGGAAGTTATTGA-3'					
Beclin1	Fwd	5'-GTGTGCAGCAGTTCAAGGAG-3'	NM_001139818.1	103	-----	-----	97
	Rev	5'-CTGCCTCCTGTGTCCTCAAT-3'					
Calpastatin	Fwd	5'-GCAAGCTGACAGAGATGGAAG-3'	NM_001173691.1	70	97	99	-----
	Rev	5'-AACCTGTACTCTGGTGGGAGA-3'					
Calpastatin	Fwd	5'-GCCGTCAAATCTGCTGCTAA-3'	NM_001173691.1	100	-----	-----	100
	Rev	5'-GCTCTGGGATAGGAGTCATGT-3'					
Calpain 7	Fwd	5'-AACAACCCTCAGTACCGGCT-3'	NM_001173603.1	100	-----	109	-----
	Rev	5'-GTGCAAAGTCATCCTTGTCAGT-3'					
Calpain 7	Fwd	5'-TTGCCTTTCCTGTTCCATTC-3'	NM_001173603.1	119	105	-----	108
	Rev	5'-GATCATGGTGGGGTTATTGC-3'					
Calpain small subunit1	Fwd	5'-TGGAGATGACATGGAGGTGA-3'	NM_001173560.1	99	107	106	110
	Rev	5'-TCAATGCTAAACCCGTCTGTC-3'					
Cathepsin D	Fwd	5'-ATCTGCCTGAGTGGCTTCAT-3'	NM_001124711.1	124	103	102	105
	Rev	5'-GTTGTCACGGTCGAACACAG-3'					
Cathepsin L	Fwd	5'-GTCAAGGACCAGGGATCATGT-3'	NM_001146546.1	120	101	97	103
	Rev	5'-GTCCACCAGGTTCTGTTCAC-3'					
DDIT3	Fwd	5'-GCGAAGAAGAGCAGGAGAGA-3'	XM_020482828.1	73	105	101	117
	Rev	5'-TCTCGTTCTGGTCCGTCAG-3'					
E1F-α	Fwd	5'-AAGGAGGTCAGCACCTACATC-3'	NC_027313.1	73	97	100	104
	Rev	5'-ATCCAGAGATGGGCACAAAG-3'					

Table S1 (continued). Primer sequences and efficiency (E) in Arctic char skeletal muscle, liver and heart

Primer	Sequence		Acc. No.	BP	Muscle E (%)	Liver E (%)	Heart E (%)
eif2α	Fwd	5'-AGATGGAGGTGTGGGATGTC-3'	NM_001140088.1	142	95	99	107
	Rev	5'-TAGCCGTTGCTGACACGTAG-3'					
Fbxo25	Fwd	5'-CCAGCTCATAGCCAGGTCTC-3'	NM_001139897.1	103	95	108	97
	Rev	5'-ATGGTCCTCCAGAACCTTCC-3'					
GAPDH	Fwd	5'-AACATCATCCCAGCCTCCAC-3'	NM_001123561.1	147	104	107	-----
	Rev	5'-GGCAGGTTTCTCAAGACGGA-3'					
HIF1a	Fwd	5'- AGCCTGCACATCCTTCTGTC-3'	NM_001140022.1	136	100	-----	98
	Rev	5'-CAGCCTCTGGTTGAGAGGTC-3'					
HIF1a	Fwd	5'- CCGTTTCCTGGCTAAGAGTG-3'	NM_001140022.1	89	-----	97	-----
	Rev	5'-CAGCCTCTGGTTGAGAGGTC-3'					
LC3A	Fwd	5'-GCCTTCTTCCTCCTGGTCA-3'	NM_001139589.1	119	101	105	106
	Rev	5'-TCCTGAGAGGCGTAAACCAT-3'					
LC3B	Fwd	5'-CAAGTTCCTGGTTCCTGACC-3'	NM_001252356.1	131		105	109
	Rev	5'-CTGCCGACACTGAGACCAT-3'					
Mafbx	Fwd	5'-AGTACCACTTCACTGACAGACA-3'	NM_001185027.1	78	100	101	103
	Rev	5'-ACATCTTCTTCCACTCCAACTG-3'					
Murf1	Fwd	5'-CTCCATGTGCAAAGTGTTCG-3'	NM_001279122.1	155	102	-----	-----
	Stem	5'-TGTCCTCCATCTGAGCCATC-3'					
rs11	Fwd	5'-ATGTCGGTCCATCTCTCACC-3'	NM_001123538.1	144	102	106	105
	Stem	5'-GAACTGCTTCTTGGCTCCAG-3'					
UBE2H	Fwd	5'-ACAGCCCTTTACGATCTCACCAAT-3'	NM_001165354	155	104	-----	109
	Stem	5'-TTCTGGATGTACTCTTTGATTTTCTG-3'					
VEGFa	Fwd	5'-GCCTTGCTCAGAGAGAAGAAAG-3'	XM_014169157.1	139	102	-----	115
	Stem	5'-CCTTGGTTTGTCACATCTGC-3'					
VEGFa	Fwd	5'-GAGCCTTGCTCAGAGAGAAGA-3'	XM_014169157.1	139	-----	98	-----
	Stem	5'-CCTTGGTTTGTCACATCTGC-3'					
VHL	Fwd	5'-CGAATCATGCGACCAGTATG-3'	XM_021569262.1	195	102	101	98
	Stem	5'-AGCCTGTCCATTCTCCATTG-3'					

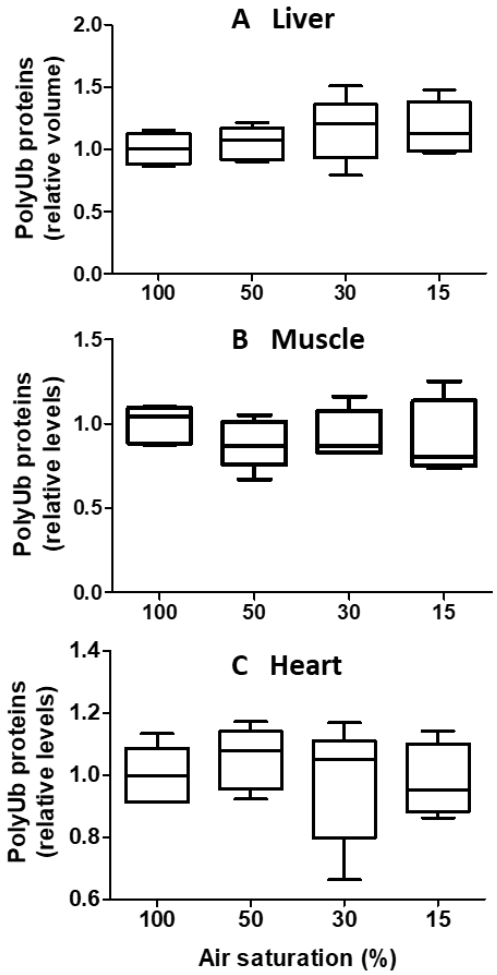

Figure S1. Polyubiquitinated proteins (relative band densities) in A) liver, B) muscle and C) heart of hypoxic Arctic char. Data are normalized to control levels and values are expressed as mean ± s.e.m.